

H α long term monitoring of the Be star β Cep Aa

G. Catanzaro*

INAF - Osservatorio Astrofisico di Catania, Via S. Sofia 78, 95123 Catania, Italy

Accepted 2008 March 27. Received 2008 March 27; in original form 2008 February 12

ABSTRACT

Recent papers published in the last years contributed to resolve the enigma on the hypothetical Be nature of the hot pulsating star β Cep. This star shows variable emission in the H α line, typical for Be stars, but its projected rotational velocity is very much lower than the critical limit, contrary to what is expected for a typical Be star. The emission has been attributed to the secondary component of the β Cep spectroscopic binary system.

In this paper, using both ours and archived spectra, we attempted to recover the H α profile of the secondary component and to analyze its behavior with time for a long period. To accomplish this task, we first derived the atmospheric parameters of the primary: $T_{\text{eff}} = 24000 \pm 250$ K and $\log g = 3.91 \pm 0.10$, then we used these values to compute its synthetic H α profile and finally we reconstructed the secondary's profile disentangling the observed one.

The secondary's H α profile shows the typical two peaks emission of a Be star with a strong variability. We analyzed also the behavior versus time of some line width parameters: equivalent width, V/R, FWHM, peaks separation and radial velocity of the central depression.

Projected rotational velocity ($v \sin i$) of the secondary and the dimension of the equatorial surrounding disk have been estimated, too.

Key words: stars: emission-line, Be – stars: individual: β Cephei – (stars:) binaries: spectroscopic

1 INTRODUCTION

The star β Cephei (HD 205021, $V = 3.2$) is well known to be the prototype of a class of hot pulsating stars. Several studies reported in the recent literature have been outlined a star oscillating with at least five frequencies: $f_1 = 5.2497104$ c d $^{-1}$, $f_2 = 5.385$ c d $^{-1}$ and $f_3 = 4.920$ c d $^{-1}$ (Aerts et al. 1994) and $f_4 = 5.083$ c d $^{-1}$ and $f_5 = 5.417$ c d $^{-1}$ (Telting et al. 1997).

Further, the star (β Cep A) is actually a complicated multiple system. In fact, beside to have a visual companion (β Cep B, $V = 7.9$) at a distance of 13.4", it is also a member of a spectroscopic system whose second star (β Cep Aa) was discovered using speckle interferometry by Gezari et al. (1972) at a distance of $\approx 0.25''$. The parameters of the close binary orbit have been determined later by Pigulsky & Boratyn (1992) combining speckle interferometry and the variations in the pulsation period, due to the so-called light time effect. Recent speckle measurements by Hartkopf et al. (2001) place the position of the companion to about 0.1" from the primary and Balega et al. (2002) found a magnitude difference of 1.8 between the two components in a red filter centered on 810 nm and 60 nm wide.

More observations are still necessary to improve the orbital solution.

Another characteristic that gives more interest to this object is the variable emission observed in the H α . Since Karpov (1933), the presence of this emission had been reported by several authors: Wilson & Seddon (1956) or Kaper & Mathias (1995), who observed a decreasing emission from 1990 to 1995. In the same years, β Cep has been observed with the coude spectrograph of the 2.6 meter telescope of the Crimean Astrophysical Observatory by Pan'ko & Tarasov (1997). Over the entire period covered by their observations, the H α was in emission with a pronounced two component structure and a small intensity above the continuum level. The same authors stated that in November 1987 the line showed an absorption profile without any sign of emission.

The kind of variable emission discussed so far is typically the characteristic of Be stars. Be stars are rapidly rotating B-type stars that lose mass in an equatorial, circumstellar disk (see the recent review by Porter & Rivinius (2003)). A general characteristic of Be stars is that they rotate very fast, typically at about 70%-80% of their critical limit ($v_{\text{crit}} = \sqrt{GM_*/R_*}$) corresponding to a several hundred of km s $^{-1}$ (Slettebak 1982). On the contrary, the pro-

* E-mail: Giovanni.Catanzaro@oact.inaf.it

jected rotational velocity of β Cep A (26 km s^{-1} , Morel et al. (2006)) is very much lower than this limit and this questions its real nature.

Hadrava & Harmanec (1996) separated emission and absorption components of the $H\alpha$ profile from their 1996 spectra and found that they move in antiphase. They speculated on two possible scenarios: *i*) the observed emission arises from reprocessing of the light originating in the stellar photosphere in an outer envelope, *ii*) the star is not a pulsating object but a rapidly rotating oblique rotator with a magnetic dipole geometry.

Recently, Schnerr et al. (2006) argued for the first time that the $H\alpha$ emission observed from the β Cep system is not related to the slowly rotating primary star, but to the secondary, being the latter a classical Be star. Unfortunately, they obtained only one spectrum at the *Nordic Optical Telescope* and, then, no conclusion about the variability of the emission could be drawn.

In this paper we try to recover the recent emission history of β Cep Aa. To achieve this goal, we firstly disentangled the spectra of the two components from the observed one. This has been done using a synthetic profile for the $H\alpha$ of β Cep A, for which T_{eff} and $\log g$ have been estimated as described in Sect. 3. Then, we analyzed the behavior with time of some $H\alpha$ width parameters like its equivalent width, the full width at half maximum, the peaks separation and the radial velocity of the central depression. Finally, we attempted to estimate the $v \sin i$ of β Cep Aa and the dimension of its surrounding disk.

2 OBSERVATION AND DATA REDUCTION

We observed β Cep for more than one year from July 2005 to November 2006. To extend our coverage to the past years, we queried various astronomical archives on the internet. At the end, we collected a number of 72 spectra covering the period from September 1993 to November 2006, for a total of more than 13 years. In the following we detailed each single observatory and instrument:

- 42 spectra have been taken from the archive of the *Ritter Observatory*, University of Toledo, OH USA, equipped with 1-m Ritchey-Chretien reflector. The echelle spectrograph is connected to the Cassegrain focus of the telescope by fiber optic cable of $200 \mu\text{m}$ diameter. The detector is a CCD manufactured by EEV with 1200×800 pixels of $22.5 \mu\text{m}$ size. The spectra used in this paper have been observed with $R \approx 26000$;
- 4 spectra have been downloaded from the *Isaac Newton Telescope* archive, three of them have been acquired with IDS spectrograph and one with MUSICOS. The lines of the Th-Ar lamp show that for all the spectra the resolution is $R \approx 33000$;
- 7 spectra have been downloaded from the archive of the Elodie@OHP 1.93 m telescope. Spectra have been reduced by the standard pipeline procedure, described in Baranne et al. (1996). Resolving power of these spectra is ≈ 42000 ;
- the 91 cm telescope of the *INAF-Osservatorio Astrofisico di Catania*, has been used by us to carried out 19 spectra of our target. The telescope is fiber linked to a REOSC echelle spectrograph, which allows to obtain $R = 20000$

spectra in the range $4300\text{-}6800 \text{ \AA}$. The resolving power has been checked using emission lines of the Th-Ar calibration lamp. Spectra were recorded on a thinned, back-illuminated (SITE) CCD with 1024×1024 pixels of $24 \mu\text{m}$ size, typical readout noise of $6.5 e^-$ and gain of $2.5 e^-/\text{ADU}$. These spectra have been extracted from a more complete set of observations (Catanzaro et al. 2008), in such a way to choose the one with the best SNR for each observing night.

The stellar spectra, calibrated in wavelength and with the continuum normalized to a unity level, were obtained using standard data reduction procedures for spectroscopic observations within the NOAO/IRAF package, that is: bias frame subtraction, trimming, scattered light correction, flat-fielding, fitting traces and orders extraction and, finally, wavelength calibration. IRAF package *rvcorrect* has been used to include the velocity correction due to the Earth's motions, all the spectra were then reduced into the heliocentric rest of frame.

3 ATMOSPHERIC PARAMETERS OF THE PRIMARY

The first task we had to asses in our study was to compute the synthetic $H\alpha$ profile of the primary component that we used in the reconstruction process of the secondary's profile. This calculation is possible if one knows the effective temperature and surface gravity of the primary component of the system.

The approach we used in this study to determine T_{eff} and $\log g$ was to compare the observed and theoretical profiles of $H\gamma$ and $H\beta$ lines by minimizing the goodness-of-fit parameter:

$$\chi^2 = \frac{1}{N} \sum \left(\frac{I_{\text{obs}} - I_{\text{th}}}{\delta I_{\text{obs}}} \right)^2$$

where N is the total number of points, I_{obs} and I_{th} are, respectively, the intensities – normalized to the continuum – of the observed and computed profiles and δI_{obs} is the photon noise. Errors in T_{eff} and $\log g$ are estimated as the variation in the parameters which increases the χ^2 of a unit.

The observed profiles presented in Fig. 1 have been calculated by averaging a number of 25 spectra collected by us during the Julian Day 2554041.45 (Catanzaro et al. 2008). Doppler correction has been applied to remove any radial velocity shift due to pulsations. This average spectrum has been used in order to improve the signal-to-noise ratio of each single exposures, in particular we obtained $\text{SNR} \approx 250$ in the continuum close to the $H\gamma$ and $\text{SNR} \approx 300$ in the continuum close to the $H\beta$.

Theoretical profiles have been computed with SYNTHE¹ (Kurucz & Avrett 1981) on the basis of ATLAS9 (Kurucz 1993) atmosphere models. To reduce the number of free parameters, the rotational velocity of β Cep A has been determined fitting the line profiles of the Si III triplet at $\lambda 4552$, 4567 and 4574 \AA . The value obtained of $v \sin i = 30 \pm 1 \text{ km s}^{-1}$ is almost coincident with the line

¹ All the Kurucz codes (ATLAS9 and SYNTHE) have been used in the Linux version implemented by Sbordone et al. (2004)

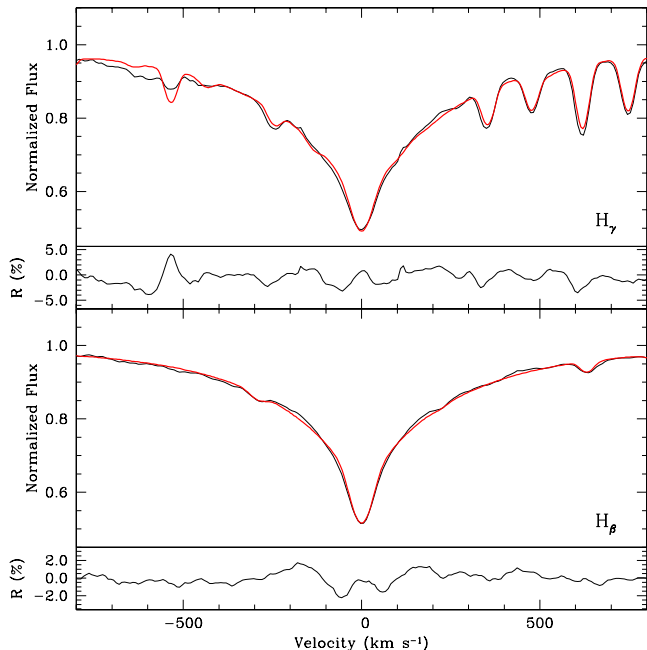


Figure 1. Comparison between observed (black) and synthetic (red) profile of H γ and H β lines. Atmospheric parameters used for this calculation are: $T_{\text{eff}} = 24000 \pm 250$ K and $\log g = 3.91 \pm 0.10$. For each Balmer line we reported also the residuals (O - C) expressed in percentage. Note the strong oxygen lines present in the wings of the H γ line.

broadening of 29 km s^{-1} measured by Morel et al. (2006) in their analysis of high resolution spectra ($R = 50\,000$).

The best fit was achieved for the following adopted parameters: $T_{\text{eff}} = 24000 \pm 250$ K and $\log g = 3.91 \pm 0.10$. In Fig. 1 we showed the comparison between the observed and computed lines profiles together with their residuals (O - C). It is interesting to note the two symmetrical bumps that appear both on the blue and red side of H β , approximately at $\pm 150 \text{ km s}^{-1}$ from the core of the line. They are located at the same velocity of the peaks observed in the H α of β Cep Aa (see Fig. 2), then they could be connected to the H β of the secondary component. On the other side, β Cep A is a non-radial pulsator, thus the peaks could be the result of the average process we undertook to recover the mean profiles used for T_{eff} and $\log g$ determination. This distortion, whatever its origin may be, could lead to a maximum error on the parameters of the order of 2 %.

In the particular case of our target, this procedure could be considered valid under the initial hypothesis that H γ and H β are not influenced by the secondary component of the binary system. As a check on the consistency of our T_{eff} and $\log g$, we estimated the abundance of silicon from lines of different ionization states. In particular we used the SiIII triplet and the SiIV $\lambda 4654 \text{ \AA}$. The abundance has been computed by means of spectral synthesis analysis using the microturbulence found by Gies & Lambert (1992), that is: $7.6 \pm 1.5 \text{ km s}^{-1}$. We derived -4.67 ± 0.08 from SiIII and -4.65 ± 0.10 from SiIV. The consistency between these two determinations convinced ourselves about the accuracy of our atmospheric parameters. As adopted Si abundance we computed the weighted average between the two previ-

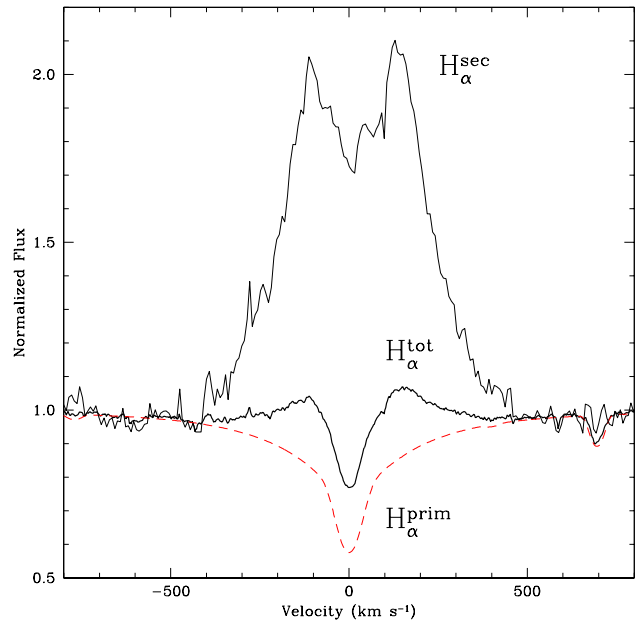


Figure 2. In this figure we illustrated the method used to recover the H α profile of the secondary. With bold solid line we represented the observed composite spectrum, with red dashed line we represented the synthetic primary component and with the normal line we indicated the reconstructed secondary profile.

ous values, that is $\log N(\text{Si})/N_{\text{tot}} = -4.66 \pm 0.06$. This abundance, that could be expressed as $\log \epsilon(\text{Si}) = 7.38 \pm 0.06^2$, is fully consistent with typical abundances for B-type field stars reported in various literature study: for instance, Dufton et al. (1990) gave $\log \epsilon(\text{Si}) = 7.5 \pm 0.2$ for both the OB associations h and χ Per and Cep OB3, Gies & Lambert (1992) found $\log \epsilon(\text{Si}) = 7.58$ from their sample of B stars and Cunha & Lambert (1994) found 7.40 ± 0.15 in a sample of B stars in the Orion association.

For the sake of comparison, we searched for other determinations of T_{eff} and $\log g$ in the literature. In particular, Heynderickx et al. (1994) found $T_{\text{eff}} = 24550$ and $\log g = 3.772$ and Niecmzura & Daaszyńska-Daszkiewicz (2005) derived $T_{\text{eff}} = 24150 \pm 350$ K and $\log g = 3.69$. As the reader can see, despite effective temperatures are perfectly consistent with our value, our gravity is ≈ 0.2 dex greater than previous determinations. Anyway, since other authors did not report their errors on $\log g$, no conclusion could be drawn about the consistency between our and literature values.

4 EXTRACTION OF THE SECONDARY SPECTRUM

The procedure we undertook to recover the H α profiles of the secondary component could be summarized as follows:

² This conversion has been calculated considering normal helium abundance.

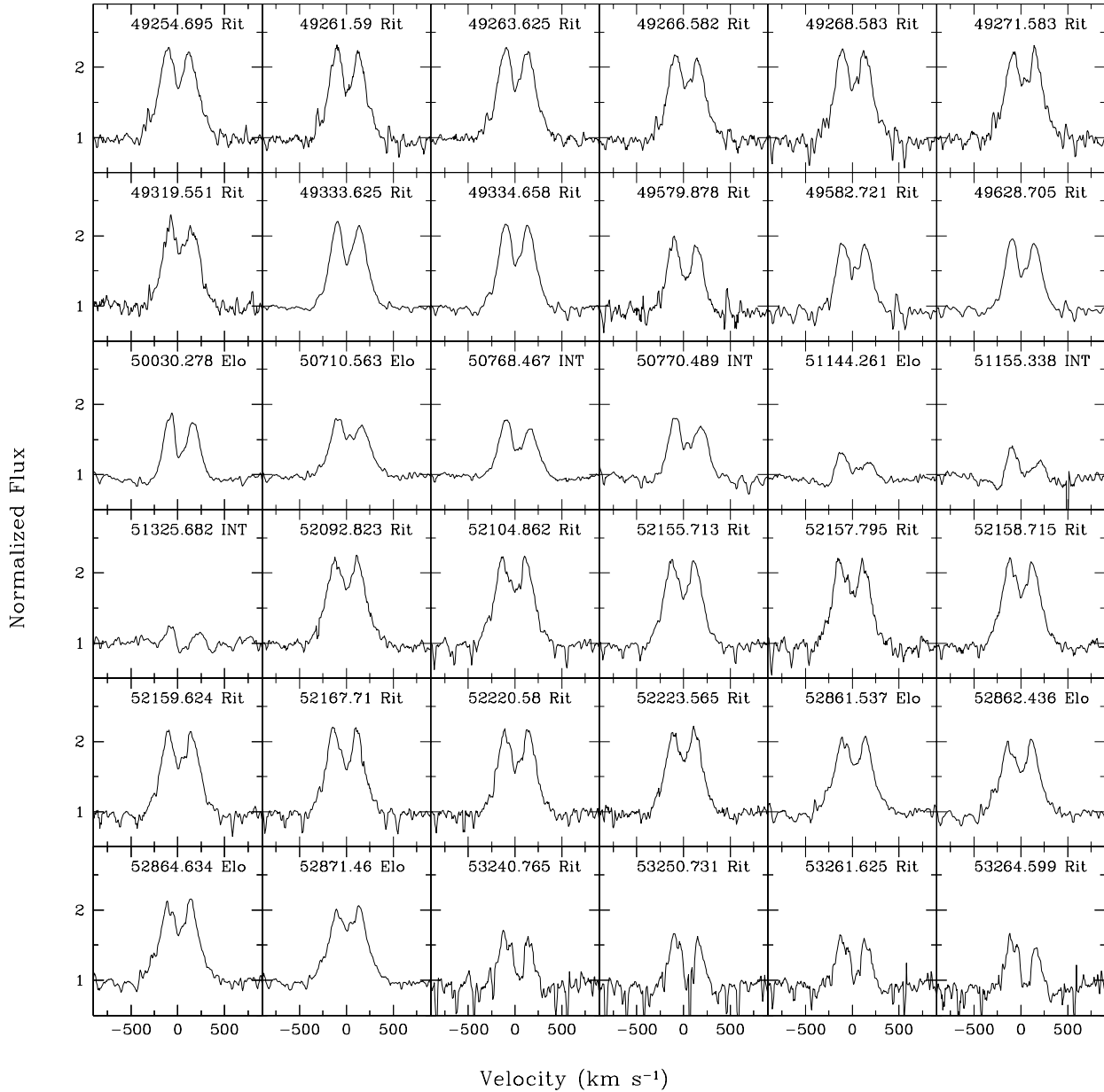


Figure 3. H α profiles of β Cep Aa reconstructed with the procedure described in the text. In each box we reported the heliocentric Julian day of the observation and a label indicating the observatory: Rit - Ritter Observatory, INT - Isaac Newton Telescope, Elo - Elodie and OAC - Catania Astrophysical Observatory.

- first, we computed synthetic H α profiles for the primary component using the atmospheric parameters derived in the previous section. Even for this line we used ATLAS9 and SYNTHE;

- then, we recovered the secondary H α line profiles from the following formula:

$$F_{\text{tot}} = \frac{F_{\text{prim}} r + F_{\text{sec}}}{1 + r} \quad (1)$$

where F_{tot} is the observed profile, F_{prim} is the synthetic H α

profile of the primary, r is the luminosity ratio between the two components computed from the magnitude difference $\Delta M = 1.8$ (Balega et al. 2002) opportunely scaled at the H α wavelength. Then from Eq. 1 it follows:

$$F_{\text{sec}} = (1 + r) F_{\text{tot}} - F_{\text{prim}} r \quad (2)$$

Since the primary component is a pulsating star with an amplitude of about 30 km s⁻¹ (Aerts et al. (1994), Telting et al. (1997), Catanzaro et al. (2008)), it has been necessary to correct the synthetic spectrum for the radial

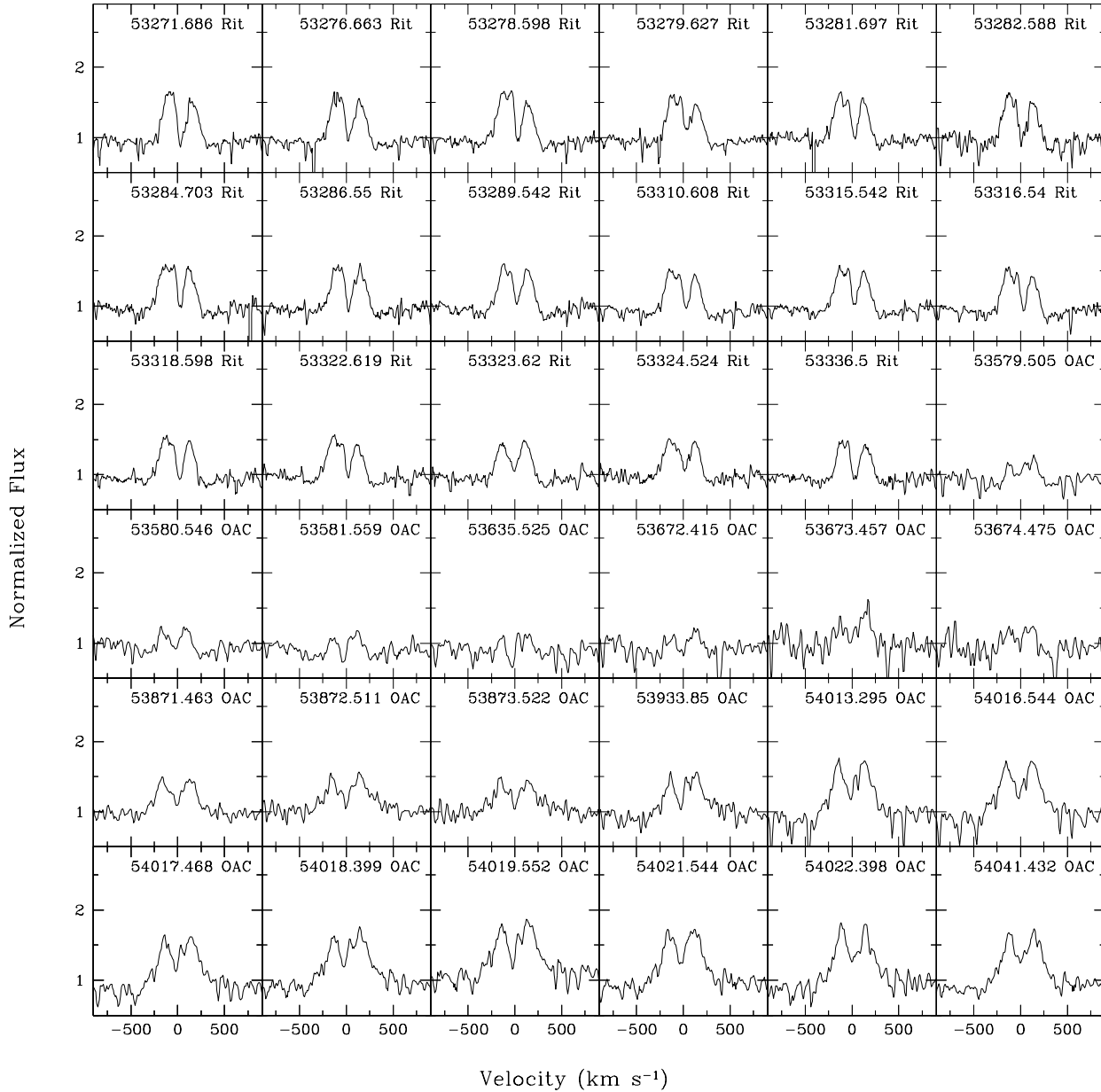


Figure 4. As in Fig. 3

velocity corresponding to the pulsating phase. For this aim we used the nearby CII doublet at $\lambda\lambda$ 6578, 6582 Å, both belonging to β Cep A. For the sake of clarity, we show in Fig. 2 an example of our procedure.

The profiles of β Cep Aa, recovered as described before and converted in the heliocentric velocity scale, are showed in Fig. 3 and in Fig. 4. Inspection of those two figures revealed the strong variability of β Cep Aa, even though no transition between shell into normal B spectrum has been observed. It always shows a double-peak symmetrical profile, with $V/R \approx 1$. Spectra are ordered by Julian Date.

5 H α VARIABILITY AND DISK PROPERTIES

In this section we analyzed the behavior with time of some line width parameters of the H α emission profile, i.e.: equivalent width (EW), the full width at half-maximum (FWHM), the peaks separation (ΔV), the radial velocity of the central depression (RV_{CD}) and the ratio of blue to red peak intensities (V/R) computed after subtraction of the continuum level³. In order to better measure positions and flux

³ Since our spectra have been normalized to the unity, we computed this ratio as $(V-1)/(R-1)$.

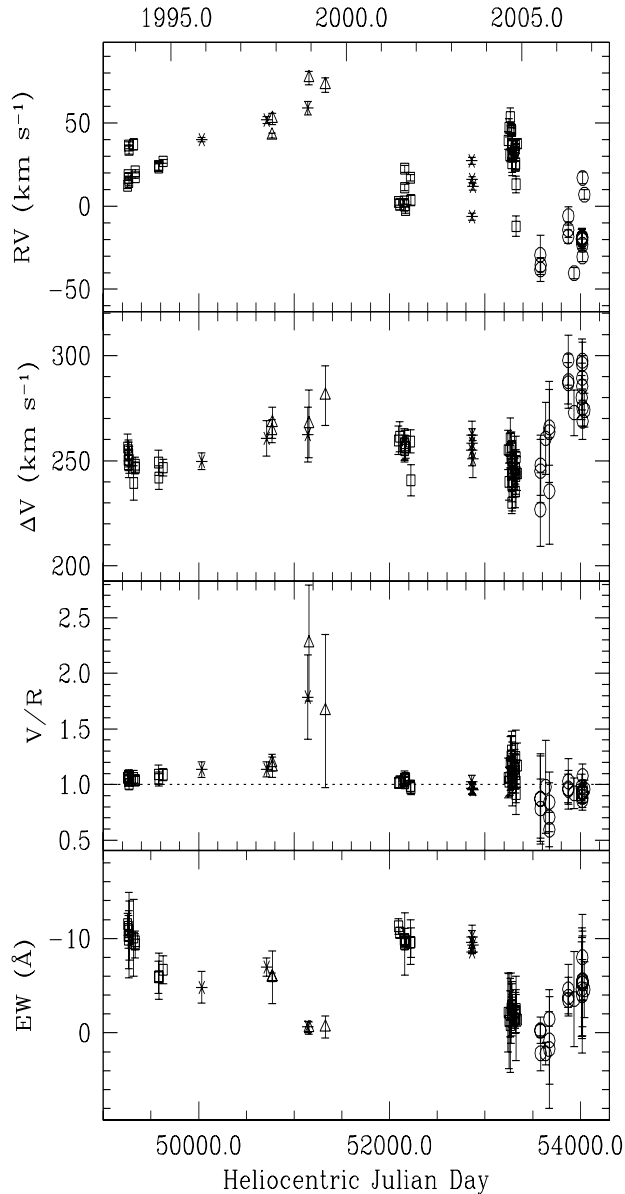


Figure 5. Variability of some quantities characteristics of the $H\alpha$ emission profile plotted in function of the Heliocentric Julian Day. From bottom to top panel: equivalent width expressed in \AA , V/R , peaks separation ΔV and radial velocities of the central depression, all expressed in km s^{-1} . Meaning of the symbols is: *squares* - data from Ritter Observatory, *triangles* - data from INT, *asterisks* - data from Elodie and *circles* - data from Catania Astrophysical Observatory. In the EW panel, the $H\alpha$ emission increase going up; the dotted line in the V/R panel represents the $V = R$ symmetry. The top axis is labeled in fraction of years.

levels of blue and red peaks, we fitted each profile with a function defined as the sum of the two gaussians centered respectively on the blue and the red peak. A similar fit has been considered to compute the radial velocity of the central depression. All this data with their relative errors have been reported in Tab. A1.

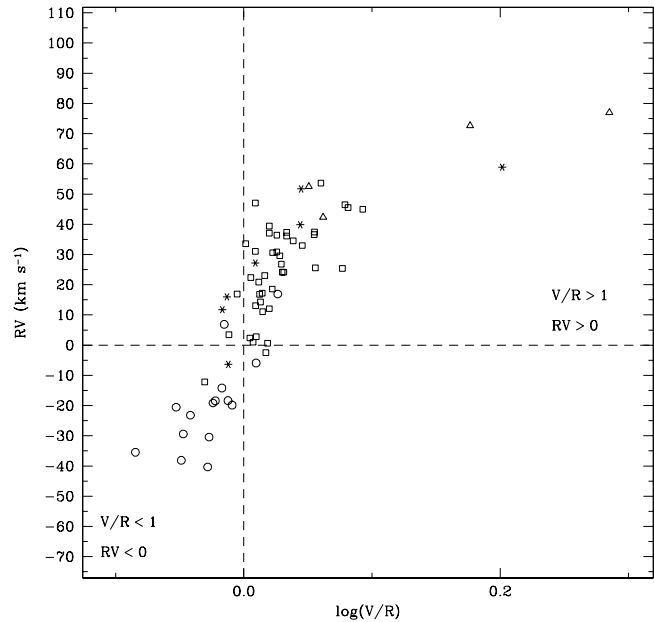


Figure 6. Correlation between V/R , expressed in logarithm, and radial velocity of the central depression.

In Fig. 5 we plotted all these quantities versus time. As a general consideration, we observed two different regimes of variations: a smoothed one between Julian Date 2449250 and 2453000 and a more rapid variation starting from $\text{JD} > 2453000$.

In the bottom panel of Fig. 5 we reported the equivalent width of $H\alpha$ versus time. By definition, it is straightforward that lines with emission profiles will have negative EW. In the plot we inverted the directions of y axis in such a way to have ascending curve in correspondence of greater emission. EW decreases from September 1993 to May 1999, then a new strong emission phenomenon occurs in July 2002 that remains constant till August 2003. Again EW decreases, it reaches a minimum during September 2005 and it increases again until November 2006, date of last spectrum of our series.

As concerns the FWHM we found its value almost constant in time, about $400 \pm 30 \text{ km s}^{-1}$, at least at the resolving power of our spectra.

The peaks separation reveled an increase from September 1993 to May 1999, then it decreased reaching a minimum in June 2005. After that date, the separation begins to increase again (third panel from bottom of Fig. 5).

The fourth panel shows the behavior of the radial velocity of the central depression. It shows a progressive red shift till May 1999. Then, we observed a blue shift till June 2005. After this date velocities present much more scatter, probably due to a worse quality of data. In general, from the variations of the radial velocity, one could draw some useful indication about the state of the disk: expanding, contracting or stationary. This is true provided that the radial velocity of the underlying star is well known. Unfortunately, since this is not possible with our data, we could not say anything about the equilibrium state of the envelope.

A similar trend has been observed for the V/R ratio, but with an exceptional increase ($V/R > 1.5$) for three julian dates: 51144.261 (Elodie), 51155.338 (INT) and 51325.682 (INT). Cyclic variability of V/R has already been observed in a number of Be stars (Hanuschik et al. 1995) and this evidence has been theoretically explained in terms of one-armed density waves precessing around the central star, the so-called Okazaki's model (Okazaki 1991). When the dense part is on the approaching side of the disk, the V peak is higher than R. On the contrary, when dense part is in the receding part of the disk, R peak will be enhanced.

It is well known from literature (see for example Hubert et al. (1987)), that in addition to the V/R variation Be stars are always accompanied by profile shifts: blueward when red component is stronger ($V/R < 1$), redward when blue component is stronger ($V/R > 1$). This feature is again explained in term of the one-armed density model as proposed by Okazaki (1996). In Fig. 6 we show the correlation between RV and V/R. It is clear that when $V/R > 1$ the profile is redshifted ($RV > 0$) and, on the contrary, the profile is blueshifted ($RV < 0$) when $V/R < 1$.

For all these quantities, we attempted to search for periodic variability using the *Phase Dispersion Method (PDM)* (Stellingwerf 1978) as coded in the NOAO/IRAF package, but no successfully results have been achieved.

Dachs et al. (1986) and Hanuschik (1986), studying the kinematics of the disks surrounding Be stars, found some useful correlations between line width parameters (in particular, FWHM and peak separation) and stellar projected rotational velocity, $v \sin i$. Later, the existence of those correlations have been confirmed by Hanuschik et al. (1988). Using those correlations, we attempted to derive the $v \sin i$ of the underlying star. In particular, Hanuschik et al. (1988) gave equations that linked each other FWHM, peaks separation and $v \sin i$ for objects whit EW of the H α emitting disk region less than 15 Å. From our measurements, we derived a velocity equal to $\approx 230 \text{ km s}^{-1}$.

The rotation law in Be star circumstellar disk is usually written as $v(r_d) \propto r_d^{-j}$, where the index $j=0.5$ if for keplerian rotation and $j=1$ for conservation of angular momentum. According to former author, the observed normalized peaks separation is a function of the outer radius of the disk, expressed in term of stellar radius, via the formula:

$$\frac{\Delta V}{2v \sin i} = r_d^{-j} \quad (3)$$

In their paper, Hanuschik et al. (1988) concluded that for their sample of Be stars the value of j is closer to 1 than to 0.5. On the contrary, Hummel & Vrancken (2000) concluded that the formation of H α shell profiles in Be stars generally requires that $j \approx 0.5$, i.e. the keplerian rotation is a valid approximation. As for our object, according to the Okazaki's model, the correlation between RV and V/R showed in Fig. 6 is a strong argument for the validity of keplerian rotation. Thus, using Eq. 3, we estimated the radius of the outer disk surrounding β Cep Aa to be $3.38 R_*$ ($j=0.5$).

6 CONCLUSION

In this paper we analyzed the last 13 years of the H α emission history of β Cep Aa. Spectroscopic data, for a total of

72 spectra, have been obtained both from *INAF - Osservatorio Astrofisico di Catania* and from archives of other three observatories as described in Sec. 2.

We used H β and H γ profiles to derive effective temperature and surface gravity of the primary. By spectral synthesis we obtained: $T_{\text{eff}} = 24000 \pm 250 \text{ K}$ and $\log g = 3.91 \pm 0.10$.

Regarding the secondary, we conclude that β Cep Aa is a Be star which shows a high degree of variability in H α emission intensity as well as in the other line width parameters here considered. From 1993 to 1999 we observed a decrease in the emission and a subsequent increase till July 2002, that remains constant till August 2003. After this long cycle extended for 10 years, we again observed a decline toward a minimum and a raise toward a new phase of strong emission, in a shorter period of about 3 years.

As concerns, V/R ratio, peaks separation and radial velocity of central depression, we also observed a long 10 years cycle out-of-phase with respect the EW and a more rapid variability occurred during the last 3 years. As for the FWHM, we did not observe any appreciable change, at least at the resolving power of our data.

Making use of some useful literature correlations between FWHM, peaks separation and stellar projected rotational velocities, we estimated for the first time the $v \sin i$ of β Cep Aa equal to $\approx 230 \text{ km s}^{-1}$ and the outer radius of the surrounding disk, $r_d = 3.38 R_*$.

ACKNOWLEDGMENTS

This research has made use of the SIMBAD database, operated at CDS, Strasbourg, France. The author wish to thanks the anonymous referee for his/her suggestions useful to improve the scientific impact of the manuscript.

A warm thanks to Anna for her contribution in improving the english form of my original manuscript.

REFERENCES

- Aerts C., Mathias P., Gillet D., Waelkens C. 1994, A&A, 286, 109
- Balega I. I., Balega Y. Y., Hofmann K.-H., et al., 2002, A&A, 385, 87
- Baranne A., Queloz D., Mayor M., et al., 1996, A&AS, 119, 373
- Catanzaro G., Leone F., Busá I., Romano P., 2008, NewA, 13, 113
- Cunha K., Lambert D. L., 1994, ApJ, 466, 170
- Dachs J., Hanuschik R., Kaiser D., Rohe D., 1986, A&A, 159, 276
- Dufton P. L., Brown P. J. F., Fitzsimmons A., Lennon D. J., 1990, A&A, 232, 431
- Gezari D. Y., Labeyrie A., Stachnik, R. V. 1972, ApJ, 173, L1
- Gies D. R., Lambert D. L., 1992, ApJ, 387, 673
- Hanuschik R. W., Hummel W., Dietle O., Sutorius E., A&A, 300, 163
- Hanuschik R. W., Kozok J. R., Kaiser D., 1988, A&A, 189, 147
- Hanuschik R. W., 1986, A&A, 166, 185
- Hadrava P., Harmanec P. 1996, A&A, 315, L401

Hartkopf W., Mason B., Wycoff G., McAlister H. 2001, Fourth Catalog of Interferometric Measurements of Binary Stars

Heynderickx D., Waelkens C., Smeyers P., 1994, *A&AS*, 105, 447

Hummel W., Vrancken M., 2000, in: *The Be Phenomenon in Early-Type Stars*, IAU Coll. 175, ASP Conf. Series, Vol. 214, M. A. Smith, H. F. Henrichs, J. Fabregat, eds.

Hubert A. M., Floquet M., Chambon M. T., 1987, *A&A*, 186, 213

Kaper L., Mathias P., 1995, in: *Astrophysical Applications of Stellar Pulsations*, ASP Conference Series, Vol. 83, 295

Karpov B. G., 1933, *Lick Observatory Bull.*, 16, No. 457, 167

Kurucz R.L., 1993, A new opacity-sampling model atmosphere program for arbitrary abundances. In: *Peculiar versus normal phenomena in A-type and related stars*, IAU Colloquium 138, M.M. Dworetzky, F. Castelli, R. Faragiana (eds.), A.S.P. Conferences Series Vol. 44, p.87

Kurucz R.L., Avrett E.H., 1981, *SAO Special Rep.*, 391

Morel T., Butler K., Aerts C., Neiner C., Briquet M. 2006, *A&A*, 457, 651

Niecmzura E., Daaszyńska-Daszkiewicz J., 2005, *A&A*, 433, 659

Okazaki A. T., 1996, *PASJ*, 48, 305

Okazaki A. T., 1991, *PASJ*, 43, 750

Pan'ko E. A., Tarasov E. A., 1997, *Astronomy Letters*, 23, 545

Pigulsky A., Boratyn D. A. 1992, *A&A*, 253, 178

Porter J. M., Rivinius T., 1993, *PASP*, 115, 1153

Sbordone L., Bonifacio P., Castelli F., Kurucz R., 2004, *Mem. S.A.It. Suppl. Vol. 5*, 93

Schnerr R. S., Henrichs H. F., Oudmaijer R. D., Telting J. H. 2006, *A&A*, 459, L21

Slettebak A., *ApJS*, 50, 55

Stellingwerf R. F., 1978, *ApJ*, 224, 953

Telting J. H., Aerts C., Mathias P. 1997, *A&A*, 322, 493

Wilson R., Seddon H., 1956, *The Observatory*, 76, 145

APPENDIX A: JOURNAL OF OBSERVATIONS

Table A1. Journal of observations. For each spectrum, ordered by heliocentric julian date (HJD) we report: the equivalent width expressed in Å, the ratio between V and R peaks, the peaks separations and the radial velocity of the central depression. The last two quantities are all expressed in km s⁻¹. The capital letter next to the HJD is a flag indicating the observatory: R - Ritter Observatory, I - INT, E - Elodie and O - Catania Astrophysical Observatory.

HJD (2400000.+)	EW (Å)	V/R	Δ V (km s ⁻¹)	RV _{CD} (km s ⁻¹)
49254.695 R	-11.5 ± 1.2	1.06 ± 0.10	256 ± 13	12.1 ± 1.4
49261.590 R	-10.3 ± 1.3	1.07 ± 0.10	250 ± 10	18.6 ± 1.4
49263.625 R	-11.3 ± 1.1	1.04 ± 0.08	255 ± 10	16.8 ± 1.1
49266.582 R	-9.9 ± 3.1	1.08 ± 0.10	248 ± 13	36.4 ± 2.0
49268.583 R	-10.3 ± 4.5	1.04 ± 0.10	253 ± 12	14.2 ± 2.0
49271.583 R	-10.9 ± 3.1	1.00 ± 0.10	250 ± 13	33.5 ± 2.3
49319.551 R	-10.1 ± 4.1	1.06 ± 0.14	239 ± 16	37.0 ± 3.1
49333.625 R	-9.7 ± 0.8	1.04 ± 0.06	247 ± 6	17.2 ± 0.5
49334.658 R	-9.4 ± 1.4	1.03 ± 0.08	248 ± 7	20.8 ± 0.8
49579.878 R	-5.9 ± 1.7	1.09 ± 0.17	249 ± 12	24.1 ± 2.5
49582.721 R	-6.0 ± 2.4	1.05 ± 0.13	242 ± 11	23.0 ± 2.2
49628.705 R	-6.7 ± 1.5	1.09 ± 0.11	247 ± 8	26.8 ± 1.1
50030.278 E	-4.8 ± 1.7	1.13 ± 0.14	250 ± 8	39.8 ± 1.2
50710.563 E	-7.0 ± 0.9	1.14 ± 0.14	261 ± 17	51.7 ± 2.1
50768.467 I	-5.9 ± 0.4	1.20 ± 0.15	264 ± 11	42.3 ± 1.3
50770.489 I	-5.9 ± 2.8	1.16 ± 0.19	268 ± 15	52.4 ± 3.3
51144.261 E	-0.6 ± 0.6	1.79 ± 0.75	262 ± 26	58.8 ± 4.0
51155.338 I	-0.5 ± 0.7	2.27 ± 1.04	268 ± 32	76.9 ± 4.0
51325.682 I	-0.6 ± 1.2	1.66 ± 1.38	281 ± 28	72.6 ± 4.3
52092.823 R	-11.3 ± 0.8	1.01 ± 0.09	260 ± 14	2.3 ± 1.7
52104.862 R	-10.6 ± 0.6	1.02 ± 0.11	261 ± 14	0.9 ± 3.2
52155.713 R	-9.9 ± 0.5	1.03 ± 0.09	255 ± 10	2.8 ± 1.6
52157.795 R	-9.6 ± 0.4	1.05 ± 0.14	257 ± 16	0.6 ± 3.6
52158.715 R	-9.9 ± 1.1	1.04 ± 0.10	256 ± 12	11.0 ± 1.9
52159.624 R	-9.4 ± 3.3	1.02 ± 0.11	258 ± 12	22.3 ± 2.0
52167.710 R	-9.7 ± 0.5	1.05 ± 0.11	257 ± 11	-2.4 ± 1.9
52220.580 R	-9.6 ± 2.4	0.99 ± 0.11	259 ± 11	16.9 ± 1.9
52223.565 R	-9.6 ± 1.6	0.97 ± 0.12	241 ± 15	3.4 ± 3.0
52861.537 E	-9.6 ± 1.2	1.03 ± 0.12	255 ± 15	27.1 ± 2.0
52862.436 E	-8.6 ± 0.1	0.97 ± 0.11	262 ± 14	-6.3 ± 2.0
52864.634 E	-10.2 ± 1.2	0.96 ± 0.10	258 ± 14	15.9 ± 1.8
52871.460 E	-9.3 ± 0.8	0.95 ± 0.10	251 ± 17	11.7 ± 2.0
53240.765 R	-2.2 ± 4.2	1.06 ± 0.36	255 ± 19	39.4 ± 5.4
53250.731 R	-1.3 ± 5.1	1.03 ± 0.26	240 ± 18	47.0 ± 5.4
53261.625 R	-2.0 ± 2.4	1.07 ± 0.33	255 ± 16	30.6 ± 3.8
53264.599 R	-0.8 ± 5.0	1.19 ± 0.49	261 ± 19	53.6 ± 5.3
53271.686 R	-2.6 ± 3.7	1.25 ± 0.36	251 ± 15	46.4 ± 3.2
53276.663 R	-2.2 ± 0.8	1.10 ± 0.24	256 ± 14	37.3 ± 2.4
53278.598 R	-2.8 ± 0.9	1.31 ± 0.34	243 ± 14	44.9 ± 1.8
53279.627 R	-2.5 ± 2.9	1.26 ± 0.34	238 ± 16	45.5 ± 3.2
53281.697 R	-2.9 ± 2.3	1.08 ± 0.18	230 ± 10	30.8 ± 2.1
53282.588 R	-2.1 ± 1.4	1.17 ± 0.42	250 ± 18	25.5 ± 5.4
53284.703 R	-2.9 ± 1.1	1.03 ± 0.44	240 ± 28	31.0 ± 12.
53286.550 R	-2.5 ± 0.6	1.10 ± 0.35	244 ± 17	36.1 ± 3.5
53289.542 R	-2.5 ± 0.5	1.08 ± 0.31	240 ± 15	29.5 ± 2.7
53310.608 R	-1.5 ± 0.9	1.14 ± 0.35	244 ± 15	32.9 ± 2.4
53315.542 R	-2.3 ± 0.3	1.12 ± 0.32	235 ± 15	34.5 ± 2.4
53316.540 R	-1.5 ± 1.0	1.17 ± 0.40	246 ± 17	36.5 ± 2.6
53318.598 R	-2.2 ± 2.2	1.09 ± 0.34	247 ± 15	24.1 ± 2.7
53322.619 R	-2.3 ± 2.3	1.25 ± 0.48	243 ± 19	25.4 ± 3.3
53323.620 R	-1.5 ± 4.5	0.92 ± 0.37	245 ± 21	-12.2 ± 6.1
53324.524 R	-2.5 ± 1.5	1.03 ± 0.38	252 ± 20	13.0 ± 5.0
53336.500 R	-1.4 ± 0.6	1.17 ± 0.40	244 ± 16	37.4 ± 2.6

Table A1 – *continued*

HJD (2400000.+)	EW (Å)	V/R	ΔV (km s ⁻¹)	RV _{CD} (km s ⁻¹)
53579.505 O	-0.3 ± 1.4	0.87 ± 0.76	227 ± 35	-29.3 ± 11.
53580.546 O	-0.2 ± 0.7	0.87 ± 0.81	245 ± 30	-38.1 ± 7.0
53581.559 O	2.2 ± 1.9	0.78 ± 0.53	248 ± 29	-35.4 ± 4.2
53635.525 O	2.2 ± 1.2	0.98 ± 0.84	261 ± 34	
53672.415 O	1.7 ± 6.3	0.71 ± 0.61	264 ± 48	
53673.457 O	-1.5 ± 0.8	0.59 ± 0.31	266 ± 36	
53674.475 O	0.8 ± 4.7	0.84 ± 0.54	236 ± 51	
53871.463 O	-3.5 ± 0.7	0.96 ± 0.26	287 ± 20	-18.3 ± 3.9
53872.511 O	-4.6 ± 2.6	0.95 ± 0.35	298 ± 24	-14.1 ± 4.6
53873.522 O	-3.8 ± 2.0	1.03 ± 0.41	288 ± 26	-5.9 ± 5.5
53933.850 O	-3.6 ± 5.0	0.92 ± 0.27	273 ± 22	-40.3 ± 3.3
54013.295 O	-4.6 ± 5.0	0.97 ± 0.23	280 ± 21	-19.8 ± 5.8
54016.544 O	-5.3 ± 5.9	0.93 ± 0.20	296 ± 24	-19.1 ± 5.2
54017.468 O	-4.0 ± 6.1	0.94 ± 0.21	285 ± 22	-18.4 ± 4.9
54018.399 O	-5.5 ± 4.8	0.86 ± 0.18	289 ± 21	-20.5 ± 4.7
54019.552 O	-8.0 ± 4.5	0.89 ± 0.19	297 ± 18	-23.1 ± 3.5
54021.544 O	-5.6 ± 2.2	0.93 ± 0.17	275 ± 17	-30.4 ± 2.9
54022.398 O	-5.2 ± 5.5	1.08 ± 0.22	269 ± 17	16.9 ± 3.5
54041.432 O	-4.6 ± 3.0	0.96 ± 0.17	274 ± 16	6.8 ± 2.9